

Supplementary Information

Physicochemical stimuli as a tuning parameter to modulate the structure, stability and release kinetics of dapsone encapsulated nanostructured lipid carriers

Rohini Kanwar,¹ Michael Gradzielski,² Sylvain Prevost,^{3*} Gurpreet Kaur,¹
Marie-Sousai Appavou⁴ and S.K. Mehta^{1*}

SANS EQUATIONS

Based on earlier models,¹ the population of large scatterers was modeled as polydisperse homogeneous spheres with a log-normally distributed radius and the population of small scatterers as core-shell monodisperse triaxial ellipsoids.

The intensity for polydisperse homogeneous spheres (I_{sphere}) and $K(Q, R, \Delta SL D)$ with radius R and $\Delta SL D$ is given by

$$I_{Sphere}(Q, R) = {}^1N_{sph} \cdot <(V_{sph} \cdot \Delta SL D)^2> \cdot P(Q) \cdot S(Q) \quad (S1)$$

where 1N , $< V_{sph} \cdot \Delta SL D >$, $P(Q)$ and $S(Q)$ are the number density of scattering particles, mean average of volume and scattering contrast multiplication factor, form factor and structure factor.

For triaxial ellipsoidal core shell micelles, $I_{ii}(Q, R, \nu)$ with a radius of rotation axis 'R' is given by:

$$I_{triaxEllSh}(Q) = \int_0^1 \int_0^1 dx dy K_{sh}^2(Q, R, R_t) \quad (S2)$$

$$K(QR) = 3 \frac{\sin QR - QR \cos QR}{QR^3} \quad (S3)$$

$$K_{sh}(Q, R, R_t) = (\eta_c - \eta_{sh}) K(QR) + (\eta_{sh} - \eta_{sol}) K(QR_t) \quad (S4)$$

$$R^2 = \left[a^2 \cos^2\left(\frac{\pi x}{2}\right) + b^2 \sin^2\left(\frac{\pi x}{2}\right) \right] (1 - y^2) + c^2 y^2 \quad (S5)$$

$$R_t^2 = \left[(a+t)^2 \cos^2\left(\frac{\pi x}{2}\right) + (b+t)^2 \sin^2\left(\frac{\pi x}{2}\right) \right] (1 - y^2) + (c+t)^2 y^2 \quad (\text{S6})$$

$$V_c = \frac{4}{3} \pi abc \quad (\text{S7})$$

$$V_t = \frac{4}{3} \pi (a+t)(b+t)(c+t) \quad (\text{S8})$$

where η_c , η_{sh} , η_{sol} are scattering length density of core, shell, and solvent, respectively. a, b, c, are the semi-axes of the elliptical core, t is the thickness of the shell. V_c and V_t are the volumes of core and total volume of the core along with the shell.

KINETIC EQUATIONS

Zero-order kinetics:

$$F = k_0 \cdot t \quad (\text{S9})$$

Higuchi kinetics:

$$F = k_H \cdot t^{1/2} \quad (\text{S10})$$

First-order / First-order exponential kinetics:

$$F = F_0 - b e^{-kt} \quad (\text{S11})$$

Hixon-Crowell model:

$$1 - (1 - F)^{3/2} = k_1 \frac{t}{3} \quad (\text{S12})$$

Square root of mass:

$$1 - (1 - F)^{1/2} = k_1 \frac{t}{2} \quad (\text{S13})$$

Three seconds root of mass:

$$1 - [(1 - F)^2]^{3/2} = k_2 \frac{t}{3} \quad (\text{S14})$$

Weibull kinetics:

$$\ln [-\ln (1 - F)] = -\beta \ln t_d + \beta \ln t \quad (\text{S15})$$

Korsmeyer-Peppas (KP)/ Power law model:

$$F = k_p t^n \quad (\text{S16})$$

where F denotes the fraction of drug released up to time t, $k_0, k_H, F_0, b, k, k_{1/3}, k_{1/2}, k_{2/3}, \beta, t_d, k_p$ are the constants of the models and n is the release exponential which characterizes the release mechanism.

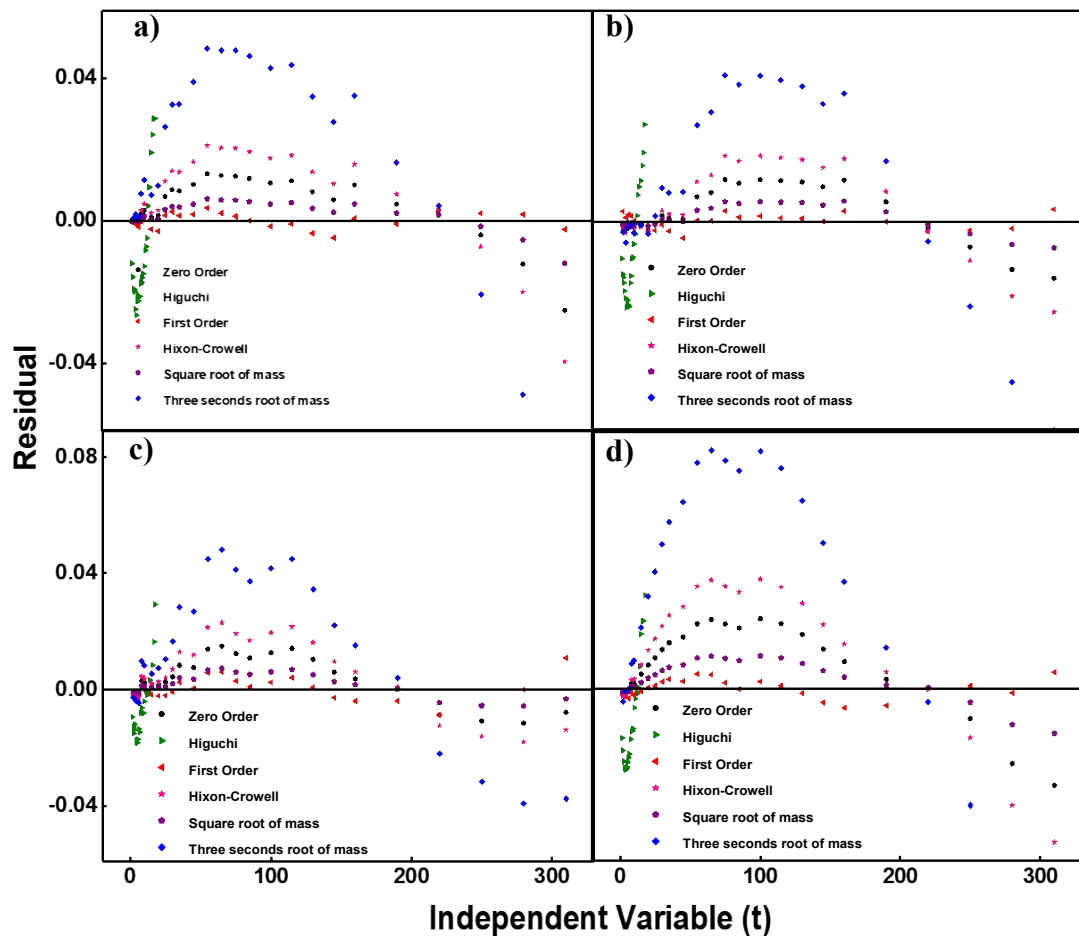


Fig. S1. a) D₁₂DAB, b) D₁₄DAB, c) D₁₆DAB and d) D₁₈DAB based NLCs *in-vitro* release profiles for Rifampicin loaded NLCs evaluated w.r.t. residuals obtained from the experimental data

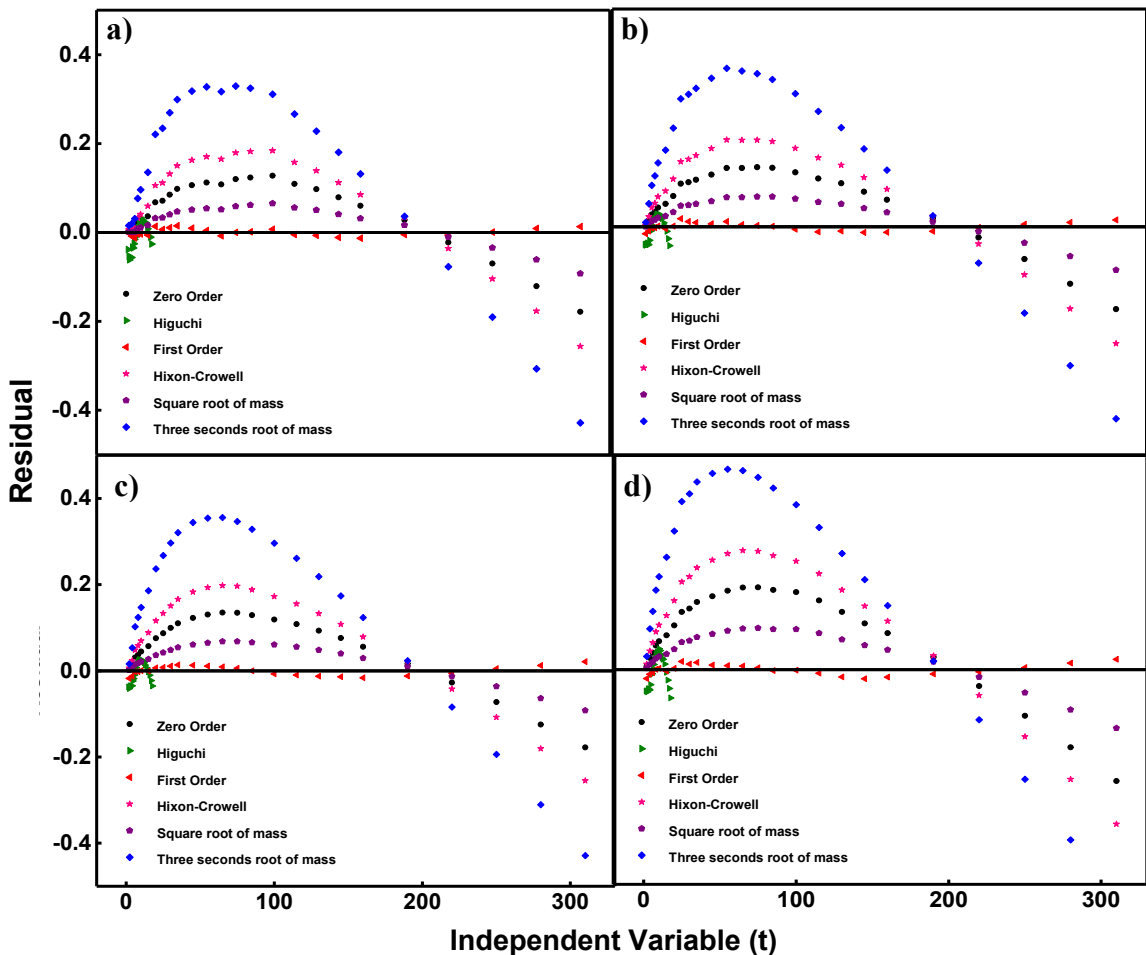


Fig. S2. a) D₁₂DAB, b) D₁₄DAB, c) D₁₆DAB and d) D₁₈DAB based NLCs *in-vitro* release profiles for Dapsone loaded NLCs valuated w.r.t. residuals obtained from the experimental data.

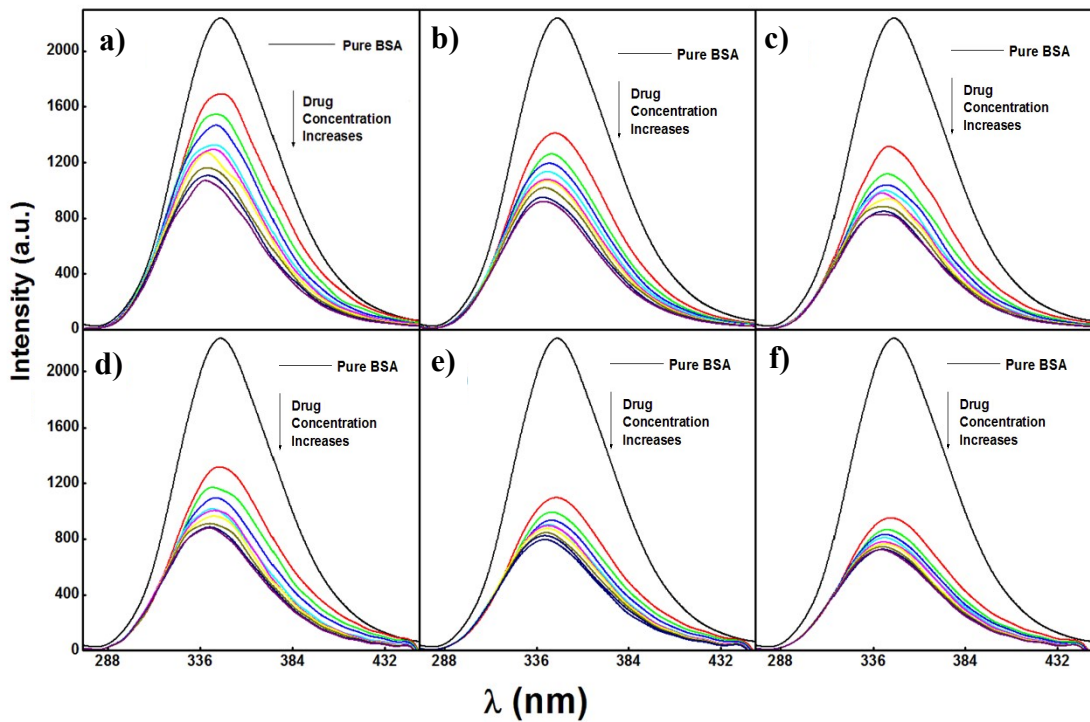


Fig. S3. Fluorescence spectra of BSA upon addition of Rifampicin encapsulated- D₁₆DAB NLCs at a) 298.15 K b) 303.15 K c) 308.15 K and D₁₈DAB NLCs at d) 298.15 K e) 303.15 K f) 308.15 K.

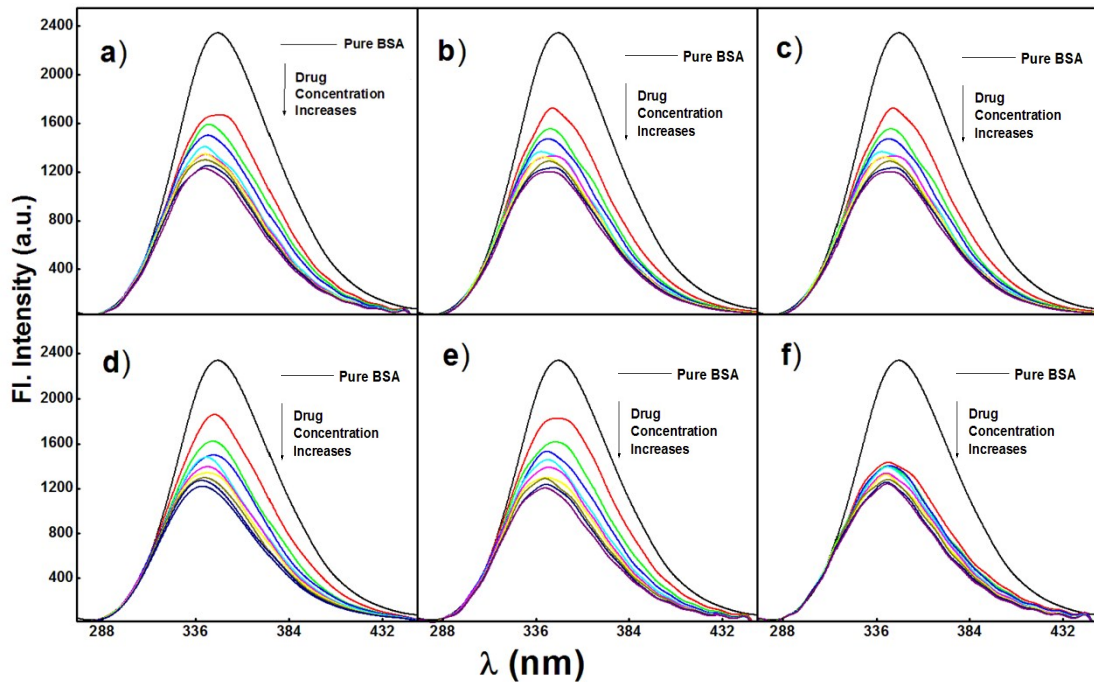


Fig. S4. Fluorescence spectra of BSA upon addition of Dapsone encapsulated- D₁₂DAB NLCs at a) 298.15 b) 303.15 K c) 308.15 K and D₁₄DAB NLCs at d) 298.15 e) 303.15 K f) 308.15 K.

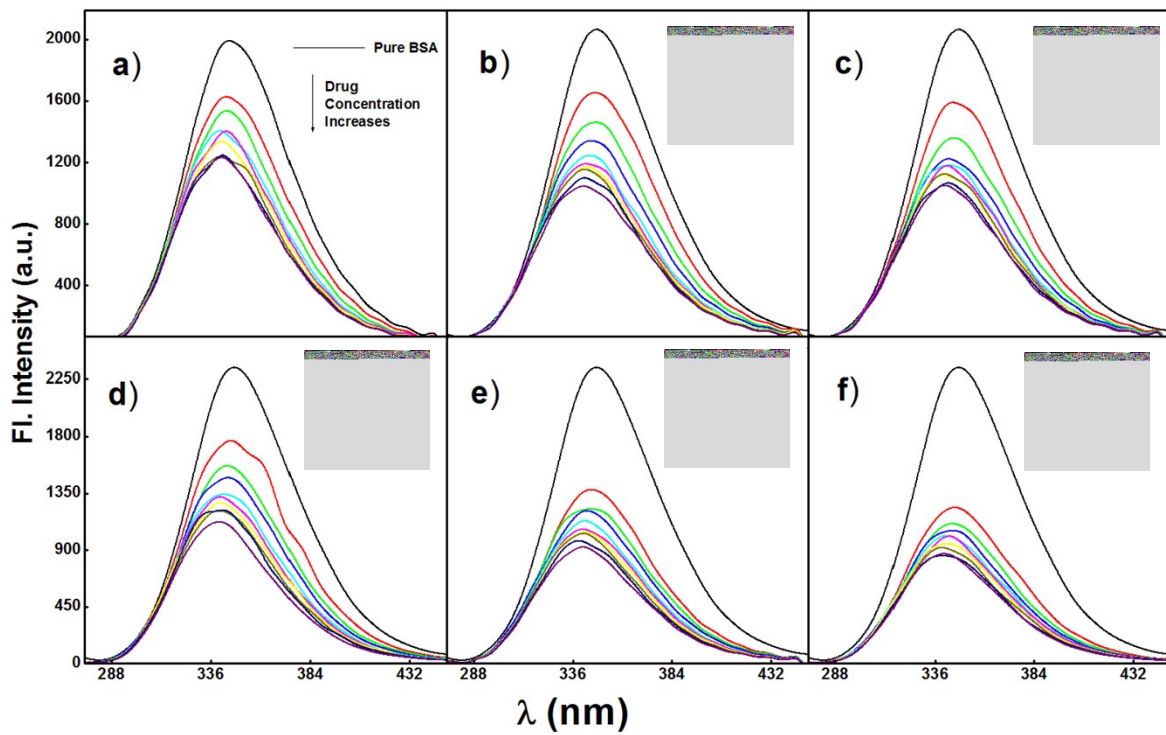


Fig. S5. Fluorescence spectra of BSA upon addition of Rifampicin encapsulated- D₁₆DAB NLCs at a) 298.15 K b) 303.15 K c) 308.15 K and D₁₈DAB NLCs at d) 298.15 K e) 303.15 K f) 308.15 K.

Table S1 Model-free analysis generated Guinier radii, forward scattering I(0), scattering contrast ΔSLD , dispersed volume fraction ϕ , the molecular weight of solid spheres M_w , scattering Invariant, porod constant, specific surface area (S/V), Porod volume and radius

Q-range	NLCs	Characteristic Parameters	0 mM	1 mM	5 mM	20 mM	50 mM	200 mM
Low Q-range	D₁₂DAB	Guinier radius (nm)	74	77	77	73	71	55
		I(0) (cm ⁻¹)	750	1087	1313	1805	2154	1341
		$M_w * 10^7$ (g/mol)	0.29	0.42	0.51	0.70	0.83	0.52
	D₁₄DAB	Guinier radius (nm)	80	85	86	81	80	65
		I(0) (cm ⁻¹)	1115	1753	2163	2919	3446	2437
		$M_w * 10^7$ (g/mol)	0.43	0.67	0.83	1.12	1.32	0.94
	D₁₆DAB	Guinier radius (nm)	83	87	91	84	81	67
		I(0) (cm ⁻¹)	1294	2075	2632	3458	3754	2540
		$M_w * 10^7$ (g/mol)	0.50	0.80	1.01	1.33	1.45	0.98
	D₁₈DAB	Guinier radius (nm)	70	73	77	72	71	66
		I(0) (cm ⁻¹)	710	1109	1508	1950	1999	1875
		$M_w * 10^7$ (g/mol)	0.27	0.43	0.58	0.75	0.77	0.72
High Q-range	D₁₂DAB	Scattering Invariant (cm ⁻¹ nm ⁻³)	0.570	0.615	0.642	0.670	0.637	0.609
		Porod constant (cm ⁻¹ nm ⁻⁴)	0.15	0.19	0.21	0.27	0.18	0.12
		Specific surface area (S/V) (nm ⁻¹)	0.86	0.95	1.02	1.28	0.91	0.60
		Porod radii (R_p) (nm)	18.4	20.3	201.3	23.3	25.1	21.8
		Porod volume (V_p) (nm ³)	25981	34858	40331	53207	66699	43475
	D₁₄DAB	Scattering Invariant (cm ⁻¹ nm ⁻³)	0.574	0.603	0.657	0.613	0.643	0.648
		Porod constant (cm ⁻¹ nm ⁻⁴)	0.136	0.151	0.228	0.125	0.193	0.170
		Specific surface area (S/V) (nm ⁻¹)	0.75	0.78	1.09	0.64	0.94	0.82
		Porod radii (R_p) (nm)	20.9	23.9	24.9	28.2	29.3	26.1
		Porod volume (V_p) (nm ³)	38337	57344	64946	94003	105780	74245
	D₁₆DAB	Scattering Invariant (cm ⁻¹ nm ⁻³)	0.565	0.648	0.670	0.661	0.679	0.658

	Porod constant (cm^{-1} nm^{-4})	0.094	0.184	0.253	0.184	0.213	0.163
	Specific surface area (S/V) (nm^{-1})	0.52	0.89	1.19	0.88	0.98	0.78
	Porod radii (R_p) (nm)	22.1	24.7	26.4	29.1	29.6	26.3
	Porod volume (V_p) (nm^3)	45215	63204	77512	103280	108990	76245
D₁₈DAB	Scattering Invariant ($\text{cm}^{-1} \text{nm}^{-3}$)	0.645	0.628	0.662	0.638	0.619	0.644
	Porod constant (cm^{-1} nm^{-4})	0.29	0.14	0.205	0.169	0.137	0.17
	Specific surface area (S/V) (nm^{-1})	1.41	0.718	0.974	0.83	0.69	0.84
	Porod radii (R_p) (nm)	18.9	23.8	24.9	27.5	28.4	25.9
	Porod volume (V_p) (nm^3)	28157	56225	64694	87082	96423	73217

Table S2 Key parameters obtained after analysis of neutron scattering data experimentally for D₁₂DAB NLCs upon electrolyte variation

Component	0 mM	1 mM	5 mM	20 mM	50 mM	200 mM
Large spheres	¹ N (*10 ⁻⁷ nm ⁻³)	0.0062	0.0062	0.0108	0.0073	0.011
	mu	14.43	15.67	13.38	19.55	18.71
	s	0.55	0.55	0.59	0.50	0.50
	<V ² >/<V> (nm ³)	747201	956854	1102449	914687	801777
	R (nm)	56	61	64	60	58
	φ _{assumed} for spheres (%)	0.05	0.06	0.12	0.07	0.09
	¹ N (*10 ⁻⁷ nm ⁻³)	136.97	147.04	149.76	147.70	146.32
Small triaxial core-shell ellipsoidal micelles	SLD _{core}	-8.30E-06	-8.30E-06	-8.30E-06	-8.30E-06	-8.30E-06
	SLD _{shell}	8.26E-05	8.26E-05	8.26E-05	8.26E-05	8.26E-05
	SLD _m	0.000584	0.000584	0.000584	0.000584	0.000584
	a	0.95	0.95	0.95	0.95	0.95
	b	2.40	2.40	2.40	2.40	2.40
	c	9.96	9.96	9.96	9.96	9.96
	t	2.27	2.27	2.27	2.27	2.27
V						
φ _{micelles} (%)						

Table S3 Model-free analysis generated Guinier radii, forward scattering I(0), scattering contrast ΔSLD, dispersed volume fraction φ, the molecular weight of solid spheres M_w, scattering Invariant, porod constant, specific surface area (S/V), Porod volume and radius.

<i>pD variation</i>							
D₁₂DAB NLCs	Characteristic Parameters	2 pD	3 pD	5 pD	7 pD	9 pD	11 pD
Low Q-range	Guinier radius (nm)	78	78	79	80	72	53
	I(0) (cm ⁻¹)	2220	1594	1323	1523	389	259
	M _w * 10 ⁷ (g/mol)	0.86	0.61	0.51	0.58	0.15	0.10
High Q-range	Scattering Invariant (cm ⁻¹ nm ⁻³)	1.08	1.14	1.05	1.04	1.06	1.09
	Porod constant (cm ⁻¹ nm ⁻⁴)	0.24	0.31	0.27	0.24	0.37	0.54
	Specific surface area (S/V) (nm ⁻¹)	0.70	0.86	0.81	0.74	1.11	1.55
	Porod radii (R _P) (nm)	21.3	18.7	18.1	19.0	12.0	10.4
	Porod volume (V _P) (nm ³)	40609	27593	24739	28807	7254	4665
	<i>Pluronic addition</i>						
D₁₂DAB NLCs	Characteristic Parameters	0 %	0.1 %	0.3 %	0.5 %	0.7 %	1 %
Low Q-range	Guinier radius (nm)	78	76	74	87	91	100
	I(0) (cm ⁻¹)	1594	1510	1526	3388	3815	4861
	M _w * 10 ⁷ (g/mol)	0.61	0.58	0.59	1.31	1.47	1.87
High Q-range	Scattering Invariant (cm ⁻¹ nm ⁻³)	1.14	1.06	1.12	1.11	1.01	1.06
	Porod constant (cm ⁻¹ nm ⁻⁴)	0.31	0.27	0.36	0.34	0.25	0.40
	Specific surface area (S/V) (nm ⁻¹)	0.86	0.82	1.02	0.97	0.78	1.18
	Porod radii (R _P) (nm)	18.7	18.9	18.6	24.3	26.1	27.8
	Porod volume (V _P) (nm ³)	27593	28219	26864	60250	74717	90516

Table S4 Key parameters obtained after analysis of neutron scattering data experimentally for D₁₂DAB NLCs upon pD variation

<i>pD variation</i>						
Component	2 pD	3 pD	5 pD	7 pD	9 pD	11 pD

Large spheres	${}^1\text{N} (*10^{-7}\text{nm}^{-3})$	0.407	1.54	0.677	0.328	0.459	1.59
	μ	17.06	11.71	13.52	16.52	11.57	8.63
	p	2.55	2.65	2.65	2.65	2.65	2.65
	s	0.72	0.66	0.66	0.66	0.66	0.66
	Average volume (nm^3)	19034	5494	8469	15446	5303	2199
	Average R (nm)	281.9	120.1	138.7	169.5	118.7	88.5
	ϕ_{assumed} for spheres (%)	0.077	0.085	0.057	0.051	0.024	0.035
	${}^1\text{N} (*10^{-7}\text{nm}^{-3})$	14.6	-	-	-	-	0.091
	μ	8.44	-	-	-	-	16.32
	p	1	-	-	-	-	1
	s	0.26	-	-	-	-	0.021
Mid sized spheres	Average volume (nm^3)	3409	-	-	-	-	18274
	Average R (nm)	13.5	-	-	-	-	16.4
	ϕ_{assumed} for spheres (%)	0.50	-	-	-	-	0.02
	${}^1\text{N} (*10^{-7}\text{nm}^{-3})$	3.58E-05	3.10E-05	2.23E-05	2.88E-05	5.59E-05	6.44E-05
	SLD_{core}	-8.30E-06	-8.30E-06	-8.30E-06	-8.30E-06	-8.30E-06	-8.30E-06
Small triaxial core-shell ellipsoidal	$\text{SLD}_{\text{shell}}$	8.00E-05	4.90E-05	4.90E-05	4.90E-05	4.90E-05	4.90E-05
	SLD_m	0.000584	0.000584	0.000584	0.000584	0.000584	0.000584
	a	0.50	1.03	1.04	1.68	0.23	0.15
	b	2.93	2.57	2.98	2.49	3.83	4.47

micelles	c	4.55	8.86	12.12	7.31	4.65	4.49
t	2.1	2.1	2.1	2.1	2.1	2.1	2.1
Average							
volume (nm ³)	28.16	98.15	157.44	128.43	17.32	12.55	
ϕ _{micelles} (%)	0.10	0.30	0.35	0.37	0.10	0.08	

Table S5 Key parameters obtained after analysis of neutron scattering data experimentally for D₁₂DAB NLCs upon addition of polymer

Pluronic addition

Component	0 %	1 %	3 %	5 %	7 %	10 %
Large spheres	${}^1\text{N} (*10^{-7}\text{nm}^{-3})$	0.442	0.600	0.823	0.196	0.151
	μ	17.65	16.59	15.67	24.71	26.44
	s	0.66	0.66	0.66	0.66	0.66
	p	2.65	2.65	2.65	2.65	2.65
	Average volume (nm^3)	18830	15629	13179	51696	63326
	Average R (nm)	181.1	170.2	160.8	253.5	271.3
	ϕ_{assumed} for spheres (%)	0.083	0.094	0.11	0.10	0.096
	${}^1\text{N} (*10^{-7}\text{nm}^{-3})$	285.413	214.107	189.014	113.458	85.9577
	SLD _{core}	-8.30E-06	-8.30E-06	-8.30E-06	-8.30E-06	-8.30E-06
	SLD _{shell}	4.90E-05	4.90E-05	4.90E-05	4.90E-05	4.90E-05
Small triaxial core-shell ellipsoidal micelles	SLD _m	0.000584	0.000584	0.000584	0.000584	0.000584
	a	0.86	0.86	0.86	0.86	0.86
	b	3.02	3.17	3.39	4.20	4.60
	c	8.44	10.54	11.43	17.07	19.95
	t	2.1	2.1	2.1	2.1	2.1
	Average volume (nm^3)	92.41	121.27	140.36	259.93	332.59
	ϕ_{micelles} (%)	0.26	0.26	0.27	0.29	0.29

Table S6 Entrapment efficiency (EE) and Loading capacity (LC) for all the NLCs at 25 °C for Rifampicin and Dapsone

NLCs	Rifampicin		Dapsone	
	EE (%)	LC (%)	EE (%)	LC (%)
D₁₂DAB	98.2± 0.18	1.44±0.05	97.1± 0.20	0.065±0.003
D₁₄DAB	98.3± 0.18	1.15±0.05	98.7± 0.21	0.055±0.003
D₁₆DAB	98.6± 0.20	1.29±0.05	98.8± 0.20	0.054±0.003
D₁₈DAB	98.2± 0.16	1.66±0.05	96.6± 0.17	0.059±0.003

Table S7 Rate constants and regression correlations {regression coefficient (R) and residual sum of squares (R')} using kinetic equations for the release of Rifampicin from D_xDAB NLCs

Kinetic Model		D ₁₂ DAB	D ₁₄ DAB	D ₁₆ DAB	D ₁₈ DAB
Zero-order kinetics	k _o	0.00071	0.00056	0.00051	0.00089
	R	0.99496	0.99444	0.99183	0.9906
	R'	0.00221	0.00152	0.00177	0.0065
Higuchi kinetics	k _H	0.00942	0.00739	0.00664	0.01191
	R	0.9797	0.97447	0.98182	0.98536
	R'	0.00884	0.00689	0.00392	0.0101
First-order exponential kinetics	k	0.00282	0.00349	0.00339	0.0041
	R	0.99939	0.99908	0.99543	0.99909
	R'	0.00011	0.00011	0.00040	0.00025
Hixon-Crowell model	k _{1/3}	0.00102	0.00081	0.000725	0.00127
	R	0.99372	0.99353	0.99085	0.9885
	R'	0.00574	0.00374	0.00423	0.01627
Square root of mass	k _{1/2}	0.00037	0.00029	0.00025	0.00046
	R	0.99608	0.99527	0.99274	0.99253
	R'	0.00046	0.00034	0.00041	0.00142
Three seconds root of mass	k _{2/3}	0.00182	0.00148	0.00134	0.0022
	R	0.98928	0.99047	0.98755	0.9813
	R'	0.03134	0.01847	0.01975	0.08068
Weibull kinetics	β	0.99413	1.10391	1.10963	1.01068
	R	0.99634	0.99441	0.96217	0.98907
	R'	0.35099	0.42091	3.72897	0.85718
Korsmeyer-Peppas (KP) model	k _k	0.00089	0.0004	0.00037	0.00113

n	0.97305	1.0831	1.0933	0.98057
R	0.99542	0.99352	0.96015	0.98676

Table S8 Rate constants and regression correlations {regression coefficient (R) and residual sum

Kinetic Model		D ₁₂ DAB	D ₁₄ DAB	D ₁₆ DAB	D ₁₈ DAB
Zero-order kinetics	k _o	0.00237	0.00236	0.00231	0.00318
	R	0.96252	0.95398	0.95474	0.95051
	R'	0.19409	0.23906	0.22479	0.46883
Korsmeyer-Peppas (KP) model	k _k	-5.06672	-4.6325	-4.52007	-4.08233
	n	0.85198	0.76702	0.73789	0.71403
	R	0.97719	0.96858	0.97421	0.97687
Higuchi kinetics	k _H	0.03313	0.0333	0.03258	0.04501
	R	0.99498	0.9964	0.99698	0.99643
	R'	0.02642	0.0190	0.01532	0.03459
First-order exponential kinetics	k	0.00987	0.011	0.01067	0.01153
	R	0.99894	0.99847	0.99797	0.99857
	R'	0.00174	0.00229	0.00286	0.00377
Hixon-Crowell model	k _{1/3}	0.0031	0.00309	0.00304	0.00392
	R	0.95262	0.94361	0.94442	0.93402
	R'	0.42539	0.51115	0.4848	0.97728
Square root of mass	k _{1/2}	0.00138	0.00136	0.00133	0.00198
	R	0.97196	0.96404	0.96475	0.96668
	R'	0.04811	0.06141	0.05714	0.11907
Three seconds root of mass	k _{2/3}	0.00433	0.00434	0.00429	0.0049
	R	0.92295	0.91304	0.91395	0.89
	R'	1.41368	1.63052	1.57557	2.73399
Weibull kinetics	β	0.93493	0.84675	0.81489	0.83671
	R	0.98567	0.97939	0.98375	0.99032
	R'	1.23549	1.47159	1.06773	0.664

of squares (R')}using kinetic equations for the release of dapsone from D_xDAB NLCs

Table S9. Composition of investigated NLCs formulations including the amount of solid lipid, amount and type of liquid lipid, type of surfactant, type of alcohol and its inference

Formulations	Amount of sophorolipid (w/w %)	Amount of liquid lipid (w/w %)	Type of liquid lipid	Type of Surfactant	Type of Alcohol
NLC-1 (Control)	40	60	Oleic acid	Tween 80	Ethanol
NLC-2	60	40	Oleic acid	Tween 80	Ethanol
NLC-3	40	60	Linoleic acid	Tween 80	Ethanol
NLC-4	40	60	Oleic acid	Tween 40	Ethanol
NLC-5	40	60	Oleic acid	Tween 80	Butanol

Table S10. Entrapment efficiency of Rifampicin (RIF) and Dapsone (DAP) loaded NLCs upon component variation

Formulation	NLC-1	NLC-2	NLC-3	NLC-4	NLC-5
D ₁₂ DAB NLCs					
EE_{RIF} (%)	98.2	98.8	96.1	97.3	93.5
EE_{DAP} (%)	97.1	98.8	95.8	96.3	95.2
R_s in nm	106.0	108.3	99.7	102.1	96.3
D ₁₄ DAB NLCs					
EE_{RIF} (%)	98.3	99.3	96.7	97.8	94.3
EE_{DAP} (%)	98.7	99.0	96.3	96.8	95.2
R_s in nm	110.4	114.1	102.1	104.1	97.2
D ₁₆ DAB NLCs					
EE_{RIF} (%)	98.6	99.7	97.4	98.4	95.2
EE_{DAP} (%)	98.8	99.5	96.8	97.1	95.7
R_s in nm	113.9	116.0	105.7	108.8	103.8
D ₁₈ DAB NLCs					
EE_{RIF} (%)	98.2	98.6	95.4	96.5	93.0
EE_{DAP} (%)	96.6	98.4	95.3	95.9	94.5
R_s in nm	99.6	106.7	95.8	97.8	90.7

Table S11. Stern-Volmer constant K_{sv} , binding constant K_b , aggregation number n, free energy change (ΔG), enthalpy change (ΔH) and entropy change (ΔS) with regression coefficients (R) for BSA-Rifampicin and BSA-Dapsone at different temperatures

Rifampicin									
$D_x DAB$	T (K)	$K_{sv} \times 10^4$ (mol ⁻¹ L)	R ²	$K_b \times 10^4$ (mol ⁻¹ L)	R ²	n	- ΔG (kJ/mol)	ΔH (kJ/mol)	ΔS (J/K mol)
12	298.15	0.097	0.99	6.82	0.98	1.40	27.58	41.91	233.20
	303.15	0.093	0.99	10.10	0.99	0.90	29.51		235.72
	308.15	0.073	0.99	14.37	0.99	0.85	29.92		233.23
14	298.15	0.104	0.98	12.85	0.99	0.99	29.15	31.35	203.04
	303.15	0.103	0.99	15.65	0.99	0.80	30.13		202.94
	308.15	0.102	0.99	19.38	0.99	0.67	31.18		203.04
16	298.15	0.112	0.98	11.50	0.99	1.03	28.88	49.98	264.62
	303.15	0.098	0.99	13.25	0.98	0.86	29.72		263.03
	308.15	0.091	0.99	22.10	0.99	0.64	31.52		264.60
18	298.15	0.090	0.98	9.55	0.98	0.78	28.57	9.74	128.57
	303.15	0.067	0.98	11.58	0.99	0.74	29.01		127.90
	308.15	0.060	0.99	13.99	0.99	0.79	29.85		128.56
Dapsone									
12	298.15	0.027	0.99	5.81	0.98	1.20	27.64	30.67	195.69
	303.15	0.025	0.99	9.19	0.98	0.77	28.32		194.70
	308.15	0.021	0.99	10.43	0.99	0.86	29.59		195.68
14	298.15	0.029	0.99	10.80	0.99	1.26	26.82	58.41	286.01
	303.15	0.027	0.99	13.24	0.99	0.86	28.71		287.53
	308.15	0.022	0.98	15.96	0.99	0.78	29.69		286.03
16	298.15	0.036	0.99	16.14	0.99	0.80	30.31	19.46	167.04
	303.15	0.033	0.99	23.67	0.99	0.54	31.30		167.55
	308.15	0.031	0.98	25.88	0.99	0.59	31.98		167.04
18	298.15	0.027	0.99	10.30	0.99	0.92	28.78	24.68	179.40
	303.15	0.023	0.99	11.20	0.99	0.88	29.42		178.54
	308.15	0.021	0.99	14.36	0.99	0.78	30.57		179.39